PAPER

Photopolymerized poly(L-lactide-*b*-*N*-vinyl-2-pyrrolidone) network resists cell adhesion *in situ*†

Yong Wang, [ab] Xiaorong Lan,[b] Shuyin Zuo,[ab] Yafeng Zou,[b] Sai Li,[*a]
Zhonglan Tang [*bc] and Yunbing Wang [b]

A three-armed star-shaped poly(L-lactide) (PLLA) oligomer was synthesized using glycerol to ring-opening and polymerize L-lactide. The resultant oligomer introduced photoreactive groups at the terminal of PLLA chains by a coupling reaction with monoethyl fumarate (FAME). Photopolymerizable resin has been prepared by mixing PLLA 3-FAME, *N*-vinyl-2-pyrrolidone (NVP) as a reactive diluent and Irgacure 2959 as a photoinitiator. The PLLA 3-FAME/NVP cross-linked network could be formed by UV curing and was characterized through mechanical property tests, cytotoxicity experiments and cell adhesion experiments. In the dry state, Young's modulus and tensile strength of the network were significantly higher than those of pure PLLA formed by fused deposition modeling (FDM) printing, due to the formation of the cross-linked net. In the wet state, however, Young's modulus and tensile strength of the network were reduced by less than those of PLLA since the water-absorbed NVP content was easy to stretch. Moreover, the resultant network not only exhibited no obvious cytotoxicity but also resisted the adhesion of L929 fibroblasts. Combined with Digital Light Processing (DLP) technology, the poly(L-lactide-*b*-*N*-vinyl-2-pyrrolidone) network may be widely used in the field of anti-adhesion barrier materials and/or biological anti-fouling materials with customization requirements.

1. Introduction

3D printing technology refers to the construction of objects based on computer control and computer-aided design (CAD) or computer tomography (CT) models, using powdered metals,[1] plastics,[2] photosensitive resins[3,4] and other materials to construct objects through a layer-by-layer manufacturing method. In the field of biomaterials, stereo lithography appearance (SLA),[5,6] digital light processing (DLP),[7,8] selective laser sintering (SLS),[9,10] and fused deposition modeling (FDM)[11,12] technologies are widely developed and applied. Among these technologies, DLP technology has the advantages of high molding accuracy, fast printing speed, and is conducive for the processing of polymer materials. The basic principle is that the digital light source is projected layer by layer on the surface of the liquid photosensitive resin in the form of surface light, and it is cured layer by layer. Gang Zhou *et al.* developed a novel personalized airway stent using light-curing acrylate resin through digital light procession three-dimensional printing technology, which shows higher accuracy and printing speed and may have the potential for customized treatment for tracheomalacia.[13] David Dean *et al.* used

poly(propylene fumarate) (PPF), titanium dioxide (TiO$_2$) as dyes, Irgacure 819 as the initiator, and diethyl fumarate (DEF) as the solvent to make a photosensitive resin, which was processed by DLP technology to manufacture tissue engineering scaffolds, which have excellent structural stability and accuracy, and can be applied to bone tissue engineering according to specific biological requirements.[14]

As kind of polyester material with good biodegradability, biocompatibility and excellent mechanical properties, poly-lactic acid (PLA) has been used in the preparation of biomedical products, such as medical sutures,[15] controlled release drug carrier,[16] fracture internal fixation,[17] tissue engineering scaffold.[18,19] However, since the hydrophobicity of the pure PLA material will make its degradation rate slow and the material brittle, it is necessary to make hydrophilic modifications to PLA in order to expand its scope of the application. Gang Xu *et al.* prepared block copolymers by copolymerization of biodegradable polymer, PLA and polyethylene glycol (PEG), where the hydrophilic chain segment improve the hydrophilicity of PLA.[20] Dana Kubies *et al.* prepared block copolymers by copolymerization of PLA and poly(ethylene oxide) (PEO), forming PEO and PLA on the surface of the polymer membrane.[21] As a hydrophilic modification material, *N*-vinyl-2-pyrrolidone (NVP) has excellent solubility and biocompatibility and has been used in the preparation of biomedical products, such as drug sustained release,[22] medical hydrogel.[23] NVP is liquid and can be widely used as a reactive diluent in the field of photosensitive resin materials.

[a]School of Chemical Engineering, Sichuan University, China

[b]National Engineering Research Center for Biomaterials, Sichuan University, China. E-mail: tang.zhonglan@scu.edu.cn

[c]Institute of Regulatory Science for Medical Device, Sichuan University, China

† Electronic supplementary information (ESI) available. See DOI: 10.1039/d1ra00554e

In this study, a photopolymerizable resin was prepared by mixing three-armed photosensitive FAME-functionalized PLLA oligomers (PLLA 3-FAME), NVP as a reactive diluent and Irgacure 2959 as photoinitiator, and the poly(L-lactide-b-N-vinyl-2-pyrrolidone) network was formed by UV curing. The mechanical strength and biocompatibility of the network obtained by UV curing were studied, comparing it to pure PLLA sheets made by FDM technology.

2. Materials and methods

2.1. Materials

L-Lactide was obtained from Jinan Daigang Biomaterial Co., Ltd. (Shandong, China) and purified by recrystallization twice from anhydrous ethyl acetate. Glycerol (Chengdu Kelong Chemical Reagent Factory, Chengdu, China), stannous octoate ($Sn(Oct)_2$) (Sigma Aldrich, Darmstadt, Germany), Irgacure 2959 (2-hydroxy-1-[4-(hydroxyethoxy)phenyl]-2-methyl-1-propanone) (Tokyo Chemical Industry, TCI, Tokyo, Japan), 4-dimethylaminopyridine (DMAP) (TCI), 1,3-dicyclohexylcar-bodiimide (DCC) (TCI), fumaric acid monoethyl ester (FAME) (TCI) and NVP (Chengdu Best Reagent Co., Ltd. Chengdu, China) were used as received. Dichloromethane (b.p. 39.8 °C) and toluene (b.p. 110.6 °C) were distilled with calcium hydride. Water used in this study was purified by a water purification system (PCDX-WJ) (Pincheng Science and Technology LTD., Chengdu, China) unless otherwise mentioned.

2.2. Synthesis of three-armed photosensitive FAME-functionalized PLLA oligomers

Three-armed PLLA oligomers (PLLA 3) were prepared using glycerol to ring-opening and polymerize L-lactide. As shown in Fig. 1A, L-lactide (225 mmol), glycerol (15 mmol), and $Sn(Oct)_2$ (7.5 mmol) as an initiator were dissolved in 65 mL of toluene in a round-bottomed flask connected with a two-way stopcock. The mixture was degassed by freeze–pump–thaw cycles five times. The radical polymerization was carried out under argon protection at 80 °C for 24 h. After the reaction, the reactant was poured into an excess diethyl ether to precipitate PLLA 3. The precipitated compound was collected over a filter and dried under vacuum. The L-lactide conversion and oligomer molecular weights were determined by ^1H NMR spectroscopy measurements.

The ^1H NMR spectra were recorded on Bruker Avance III HD 400 MHz spectrometer in deuterated chloroform ($CDCl_3$) solution with tetramethylsilane (TMS) as the internal standard. Chemical shifts (δ) were expressed in ppm.

Three-armed photosensitive FAME-functionalized PLLA oligomers (PLLA 3-FAME) were prepared by esterifying PLLA 3 with FAME to introduce functional groups at the end of PLLA chains. As shown in Fig. 1B, purified PLLA 3 (1 mmol) and FAME (6 mmol) were dissolved in 180 mL of dry DCM in a three-necked round-bottom flask connected with two two-way stopcock and a dropping funnel and stirred at 0 °C for 30 min. DCC (6 mmol) as a coupling agent and DMAP (0.2 mmol) as a catalyst were dissolved in 30 mL of dry DCM and dropped in the former solution at 0 °C. The mixture was stirred under argon protection for 48 h. The formed dicyclohexylurea was removed by filtration, and PLLA 3-FAME was purified by precipitation in methanol. The structure and degrees of functionalization of macromonomers were confirmed by ^1H NMR spectroscopy measurement.

2.3. Determination of PLLA molecular weight and polydispersity index

The number-average molecular weights (M_n) of PLLA 3 and PLLA 3-FAME, and their polydispersity (M_w/M_n) were
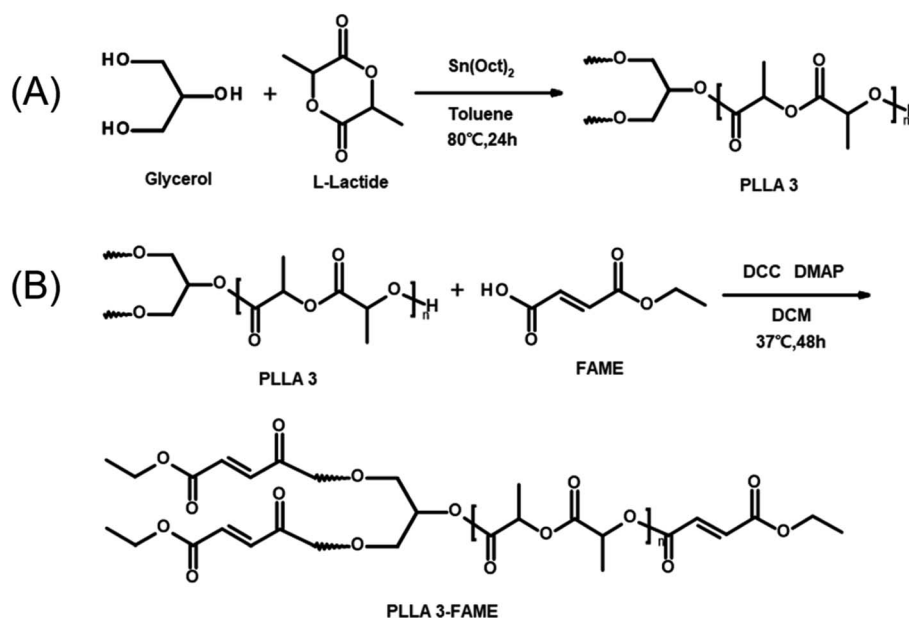

Fig. 1 Preparation of three-armed PLLA oligomers (A) and three-armed photosensitive FAME-functionalized PLLA oligomers (B).

determined by gel permeation chromatography system (GPC) in chloroform. The GPC measurements were run on a high-performance liquid chromatography instrument (Agilent 1260 Infinity). PLLA 3 and PLLA 3-FAME powders were dissolved in chloroform solution to form a polymer solution. Monodisperse polystyrene standards were used for calibration, and HPLC grade chloroform was used as the eluent. The injection volume was 30 μL, the flow rate was 1 mL min^{-1}, the temperature was set to 35 °C, and a refractive index detector (RID) was used.

2.4. Formulation of photosensitive resin and preparation of network

The resultant PLLA 3-FAME and NVP as reactive diluents were mixed with different weight ratios (PLLA 3-FAME : NVP = 45 : 55 and 50 : 50). Irgacure 2959 as a biocompatible UV photoinitiator (5 wt% of the mixture) was added to the mixture to formulate the photosensitive resin. Hereinafter, the photosensitive resins with two weight ratios were simply referred to as P45N55, P50N50.

After 30 min degassing in a vacuum, the photosensitive resin was spread on a Teflon® mold. Photopolymerization was carried out by exposing specimens cast with 365 nm UV-light for 180 s (Ultralum crosslinking cabinet, intensity 50 mW cm^{-2}) (Fig. 2A). Finally, dumbbell-shaped test specimen (5 cm × 1 cm × 0.1 cm, length × width × thickness) and the specimen sheets (1 cm × 1 cm × 0.05 cm, length × width × thickness) were obtained (Fig. 2B). Resultant samples were washed 3 times with

ethanol, and then extensively with purified water to remove unpolymerized components and impurities. PLLA sheets prepared by FDM (ESI†) were used as a control sample.

2.5. Characterization of the cross-linked network

2.5.1. Water contact angle (WCA) and water absorption measurements. The surface wettabilities of PLLA, P45N55 and P50N50 were estimated by measuring static WCA by the sessile-drip method at room temperature. Static WCAs on specimen sheets were measured using a contact angle goniometer (Theta Lite, Biolin). Water drops with 5 μL volume were generated with an electronic micrometric syringe and carefully deposited on the surface of the sample and the contact angle value was acquired within the following 30 s (the shape of the drops was stable in that period). The collected information was analyzed using the OneAttension software. The results are expressed as the average ± experimental standard deviation of at least five measurements recorded in different regions of the samples.

For the water absorption measurement, the specimen sheets of PLLA, P45N55 and P50N50 were weighed (m_0) and equilibrated in distilled water for 1 day. The specimen sheets were taken out of the water, blotted dry and weighed again (m_1). The water absorption was calculated using
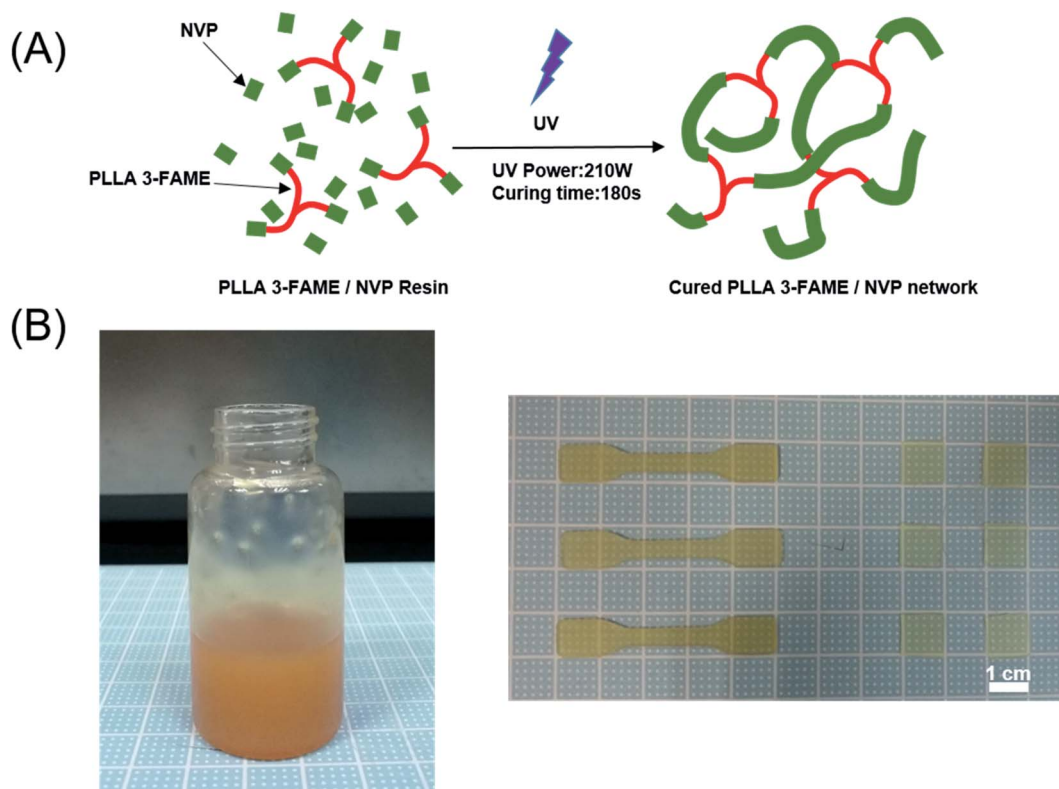
$$\text{Water absorption} = (m_1 - m_0)/m_0 \times 100\%$$

Fig. 2 (A) Three-armed FAME functionalized PLLA oligomers can be combined with a reactive diluent NVP and a photoinitiator to form a bio-absorbable biomaterial resin that can be polymerized by exposure to UV light. (B) The dumbbell-shaped test specimen and the specimen sheets was obtained after the photosensitive resin prepared in the laboratory was cured using UV (scale bar = 1 cm).

2.5.2.   Mechanical testing. The dumbbell-shaped test specimen was subjected to uniaxial tensile tests using a universal testing machine (Instron 3366, Instron Co., Ltd., U.S.A.) equipped with a 1000 N load cell. The total length of the dumbbell-shaped test specimen was 5 cm, the width of the upper and lower clamps of the machine was 1 cm, the length of the middle test part was 15 mm, and the sample was stretched at a crosshead speed of 5 mm min^{-1}. At least 10 dumbbell-shaped test specimens from two different photosensitive resins P45N55, P50N50 were used and averaged. Young's modulus was determined from the slope of the linear region of the stress–strain curve.

2.6.   Cell culture

L929 mouse fibroblast cells (MFCs) were used in this study. MFCs were cultured on tissue culture polystyrene (TCPS) dishes with Dulbecco's modified Eagle's medium (DMEM) (Gibco, Thermo Fisher Scientific, Inc., Waltham, MA) supplemented with 10% fetal bovine serum (FBS) (Gibco), 100 units per mL penicillin and 100 mg mL^{-1} streptomycin (Gibco) under a humidified atmosphere of 5.0% CO_2 at 37 °C. Subconfluent MFCs on TCPS dishes were recovered by treatment with 0.25% trypsin–2.65 mmol L^{-1} EDTA (Gibco) in PBS solution and were subcultured on 96-well or 24-well plates. MFCs with passage numbers from 18 to 23 were used for experiments.

2.6.1.   Cytotoxicity assay. The material extract for cytotoxicity assay was prepared according to the international standard ISO 10993-12:2012. Namely, six specimen sheets (1 × 1 × 0.05 cm) of PLLA, P45N55 and P50N50 were immersed in 4 mL of Dulbecco's modified Eagle's medium (DMEM) supplemented with 100 units per mL penicillin and 100 mg mL^{-1} streptomycin

with an extraction ratio of 3 cm^2 mL^{-1} and incubated for 1 and 3 days at 37 °C. Each material extract was added to 10% v/v FBS to configure the cell culture medium.

MFCs were seeded in a 96-well plate at a final cell density of 3 × 10^4 cells per well and incubated for 6 h under a humidified atmosphere of 5.0% CO_2 at 37 °C. After confirming that the cells completely adhered to the surface of the well plate, the original cell culture medium in the 96-well plate was replaced by the material extract with FBS. MFCs were cultured for 1, 3 and 5 days under a humidified atmosphere of 5.0% CO_2 at 37 °C. 96-well plates were taken at each time point, 10 μL of CCK-8 indicator was added to each well, and the absorbance at 450 nm was measured using a microplate reader.

In order to further observe the growth morphology of MFCs under the culture of the material extract, MFCs were cultured in a 24-well plate with 1 and 3 days of material extract. Similarly, MFCs were seeded in a 24-well plate at a final cell density of 3 × 10^4 cells per well and incubated for 6 h. After MFCs adhered to the surface of the well plate completely, the original cell culture medium was replaced by the material extract with FBS. The cells were cultured for 1, 3 and 5 days under a humidified atmosphere of 5.0% CO_2 at 37 °C. The growth morphology of MFCs at each time point was observed using a microscope and photographed.

2.6.2.   Cell adhesion and proliferation. The specimen sheets PLLA, P45N55 and P50N50 were sterilized under UV light for 30 minutes on each side and put into the well of the 24-well plate. A stainless ring was placed on the sheet as weight. MFCs were seeded in each well plate with specimen sheets at a final cell density of 3 × 10^4 cells per well. As a control group, MFCs were seeded in the well without specimen sheets at the same density.
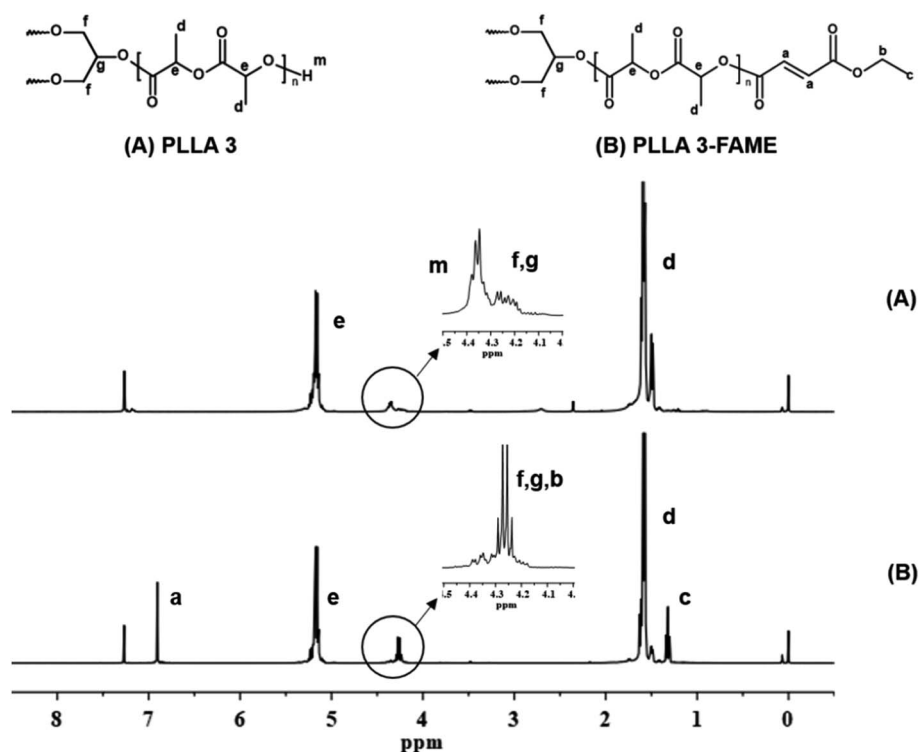

Fig. 3   (A) ^{1}H NMR spectrum of PLLA 3. (B) ^{1}H NMR spectrum of PLLA 3-FAME.

Table 1 Chemical properties and degrees of functionalisation (DF) of PLLA 3 and PLLA 3-FAME

	$M_n{}^a$	$M_n{}^b$	DF^a (%)	Yield	PDI^b
Three-armed PLLA oligomers (PLLA 3)	3400	4500	—	55%	1.17
Three-armed FAME-functionalized PLLA oligomers (PLLA 3-FAME)	3700	5700	97%	70%	1.18

^{a} Measured by NMR. ^{b} Measured by GPC.

Fig. 4 Image of the water contact angle of PLLA and the UV-cured specimen sheets P45N55 and P50N50.

After cultivation for 1 day and 3 days, cells seeded on the surface of the specimen sheets P45N55, P50N50, PLLA and TCPS were fixed with 4% paraformaldehyde and were permeabilized with Triton X-100 (1% in PBS), then were stained with DAPI (2 µg mL^{-1} in PBS) and TRITC phalloidin (100 nM in PBS) to observe the nucleus and actin cytoskeleton, respectively. The cells on the surface of the specimen sheets were observed under a magnification of 100× using a confocal fluorescence microscope.

3. Results and discussion

3.1. Synthesis of PLLA 3-FAME

Three-armed PLLA oligomers (PLLA 3) were obtained by ring-opening polymerization of L-lactide with glycerol as a trifunctional initiator. The yield of the PLLA 3 product was about 55%.

In the NMR spectrum of PLLA 3 shown in Fig. 3(A), based on the peak areas of protons (f, g, 4.17–4.30 ppm) on the glycerol skeleton and terminal protons (m, 4.30–4.4 ppm), the sum of the peak areas represents 8 hydrogen atoms, and the peak area of the –COCH– proton (e, 5.15 ppm) in the repeating unit was determined, thereby obtaining a degree of polymerization n. Using n, the arm length (expressed as the number average molecular weight of each arm) was calculated, as a result, the number average molecular weight of the prepared three-armed oligomers PLLA 3 was 3.4×10^3 g mol^{-1}. PLLA 3 were esterified with FAME, and an active

double bond was introduced at the terminal of PLLA 3 to obtain the three-armed photosensitivity FAME-functionalized PLLA oligomers (PLLA 3-FAME). The yield of PLLA 3-FAME was about 70%. Through the NMR spectrum of PLLA 3-FAME of Fig. 3B, the coupling process was confirmed by the appearance of –CH=CH– (a, 6.90 ppm). In the partially enlarged view of Fig. 3, the peak area of the terminal proton (m, 4.35 ppm) was observed to decrease, and the peak area of –CH$_2$– (b, 4.27 ppm) was increased. It was found that the terminal proton of PLLA 3 was replaced by FAME. This phenomenon further proves the completion of the coupling process. From the peak areas (d) and (c), the degree of functionalization can be calculated to be about 97%. The number-average molecular weights (M_n) of PLLA 3 and PLLA 3-FAME, and their polydispersity (M_w/M_n) were determined by gel permeation chromatography system (GPC) in chloroform. The GPC data results are shown in Table 1.

3.2. Physicochemical characterization of the cross-linked network

The photosensitive resin was prepared by mixing PLLA 3-FAME powder, the active solvent NVP and Irgacure 2959 as a biocompatible initiator. Upon irradiation, the initiator molecules decompose into free radicals, which initiate the addition copolymerization of FAME-end-groups and NVP diluent, resulting in a PLLA 3-FAME/NVP cross-linked network.

Table 2 Tensile properties of the dumbbell-shaped test specimen P45N55 and P50N50 in the dry state and after equilibration in water

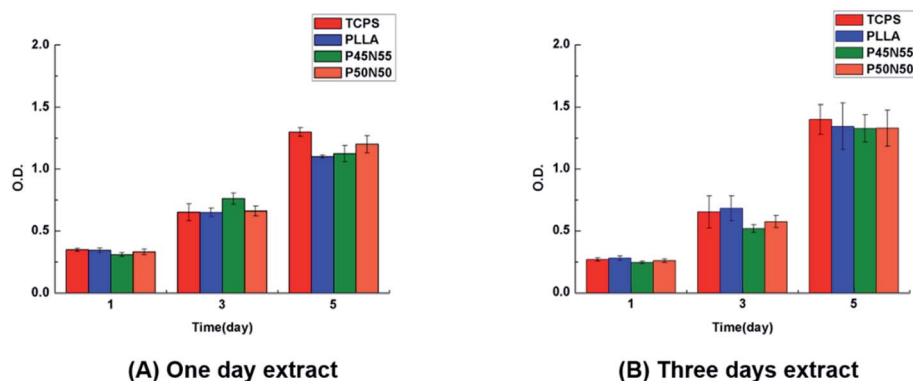| Samples	Dry/wet	Water absorption (%)	Young's modulus (MPa)	Tensile strength (MPa)	Elongation (%)
PLLA	Dry	—	969 ± 38	28 ± 3	3.82 ± 0.1
P45N55	Dry	—	1406 ± 74	77 ± 3	13.35 ± 1
P50N50	Dry	—	1262 ± 99	79 ± 5	11.02 ± 0.7
PLLA	Wet	0.43	910 ± 53	17 ± 6	3.37 ± 1
P45N55	Wet	35	82 ± 7	5 ± 1	8.93 ± 2
P50N50	Wet	29	114 ± 8	9 ± 0.5	13.73 ± 2

Fig. 5 (A) The L929 fibroblasts cultured in the one-day material extract proliferated for one day, three days, five days. PLLA and TCPS were used as controls. (B) The L929 fibroblasts cultured in the three-day material extract proliferated for one day, three days, five days. PLLA and TCPS were used as controls.

As shown in Fig. 4, in the water contact angle test, the wettability of the PLLA 3-FAME/NVP network was observed to be lower than that of pure PLLA. The water contact angle of PLLA was $91° \pm 2°$, and the water contact angles of the UV-cured specimen sheets P45N55 and P50N50 were $75° \pm 4°$ and $83° \pm 1°$, respectively. The wettability of networks decreased with NVP content increased.

Biomaterials used in surgical treatment can absorb large amounts of water, during implantation in humans. To investigate the effect of water absorption on the characterization of the PLLA 3-FAME/NVP network, samples were analyzed after drying

and after equilibration in water. The water absorption and tensile properties are listed in Table 2.

In the water absorption test, PLLA 3-FAME/NVP cross-linked network absorbed more water than the PLLA. Due to the hydrophilic character of NVP, the water absorption of the network increases with increasing NVP content.

In the dry state, Young's modulus, tensile strength and elongation of the PLLA 3-FAME/NVP network increased by introducing NVP, which is significantly higher than that of pure PLLA formed by FDM. When PLLA 3-FAME was copolymerized with NVP, the macromonomer underwent a radical-type
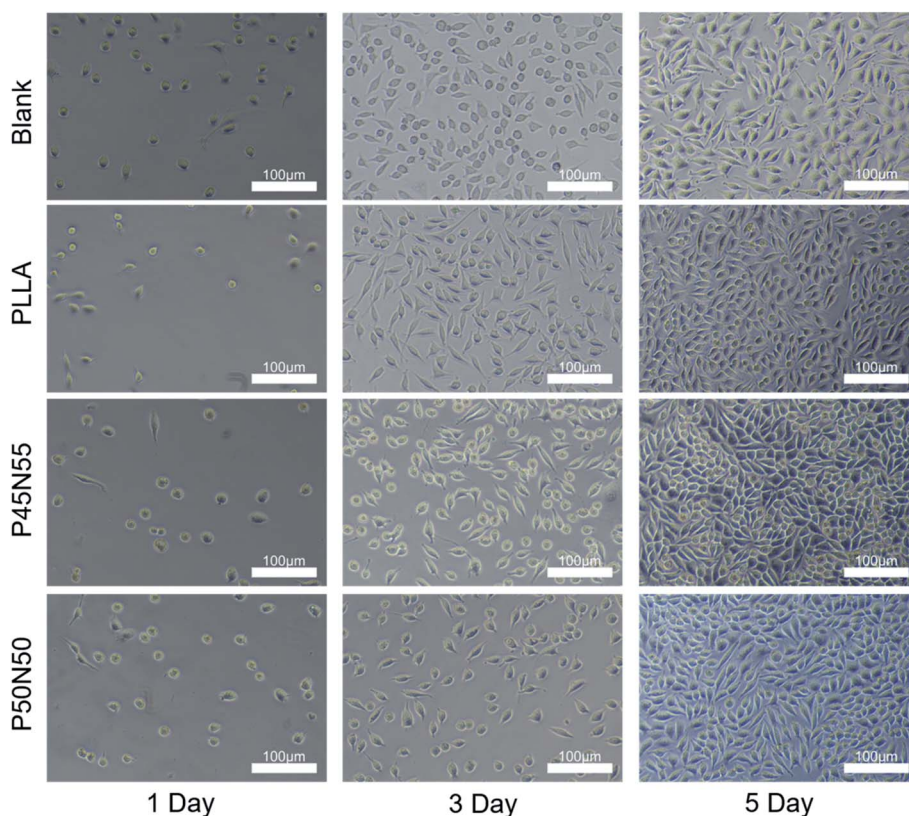

Fig. 6 The L929 fibroblast's growth morphology cultured in three-day material extract for one day, three days, five days. PLLA and TCPS were used as controls (scale bar = 100 μm).

addition reaction to form a cross-linked net. Compared with the linear PLLA macromolecular chain, the formation of the cross-linked net enhanced all of the mechanical properties. In the wet state, this trend is different, because the network containing NVP could absorb a large amount of water. The presence of water molecules makes the NVP chain within the cross-linked net easy to stretch. As a result, in the wet state, Young's modulus and tensile strength of the PLLA 3-FAME/NVP network was less than that of PLLA, which decreased significantly with increasing NVP content. However, no obvious change in the elongation was observed between the dry and wet state, due to the structure of the cross-linked net kept constant. Meanwhile, pure PLLA hardly absorbed water and exhibited a minimum difference in mechanical properties between the dry and wet states.

3.3. *In vitro* evaluation of UV-cured specimen sheets

The extracts of the UV-cured specimen sheets were soaked for 1 day and 3 days and used to cultivate L929 fibroblasts. After culturing for 1, 3, and 5 days, it can be seen that the number of cells is gradually increasing with time, and the cell proliferation rate is basically the same as that of PLLA and TCPS, indicating that there is no leaching of the cytotoxic compound (Fig. 5). To further observe the growth morphology of the cells in the culture dish under the culture of the extract, we selected the 3 day-soaked extract to culture L929 cells. Compared with the blank group and PLLA, with the extension of the culture time, the number of cells increased, the growth morphology was good, and the material were further tested for non-cytotoxicity (Fig. 6).

To evaluate cell adhesion and proliferation on the surface of resultant networks, L929 fibroblasts were cultured on specimen sheets directly. After 1d and 3d incubation, the specimen sheets were recovered and stained with DAPI and TRITC phalloidin, which were used to label the nucleus and cytoskeleton of cells on the materials, respectively. As shown in Fig. 7, after 1d culture, some of the L929 fibroblasts adhered and spread on the surface of PLLA, which is less than that on TCPS. Moreover, as shown in the upper right corner image, the cells on the surface of PLLA achieved a spindle shape, which was similarly observed on TCPS. After 3d incubation, the number of cells on the surface of PLLA increased significantly, and all the cells were observed with a spindle shape. These results suggest that L929 fibroblasts could adhere and spread on PLLA, and proliferate. In contrast, cells barely adhered on the surface of P45N55 and P50N50 after 1d culture, which was significantly less than that on PLLA. After 3d incubation, though a few cells were observed on the surface of P45N55 and P50N50, cells achieved a spherical shape, which indicates a weak adhesion and spreading of cells. These results indicate that the PLLA 3-FAME/NVP network could not be suitable for cell adhesion and proliferation. Protein adsorption on the surface of the material is considered to be the first and critical step to induce cell adhesion, spreading and proliferation. When the biological material is in contact with the physiological environment, the protein in the body will first be adsorbed on the surface of the material,[24] and then the cells interact with the proteins (such as fibronectin or vitronectin) adsorbed on the surface of the material through the integrin on the membrane to achieve cell adhesion and reproduction.[25,26] The improvement of the hydrophilicity of the material surface can effectively resist the nonspecific adsorption of proteins.[27–29] Hydration layer theory believes that the surface of polyvinylpyrrolidone (PVP) can form a stable and dense water
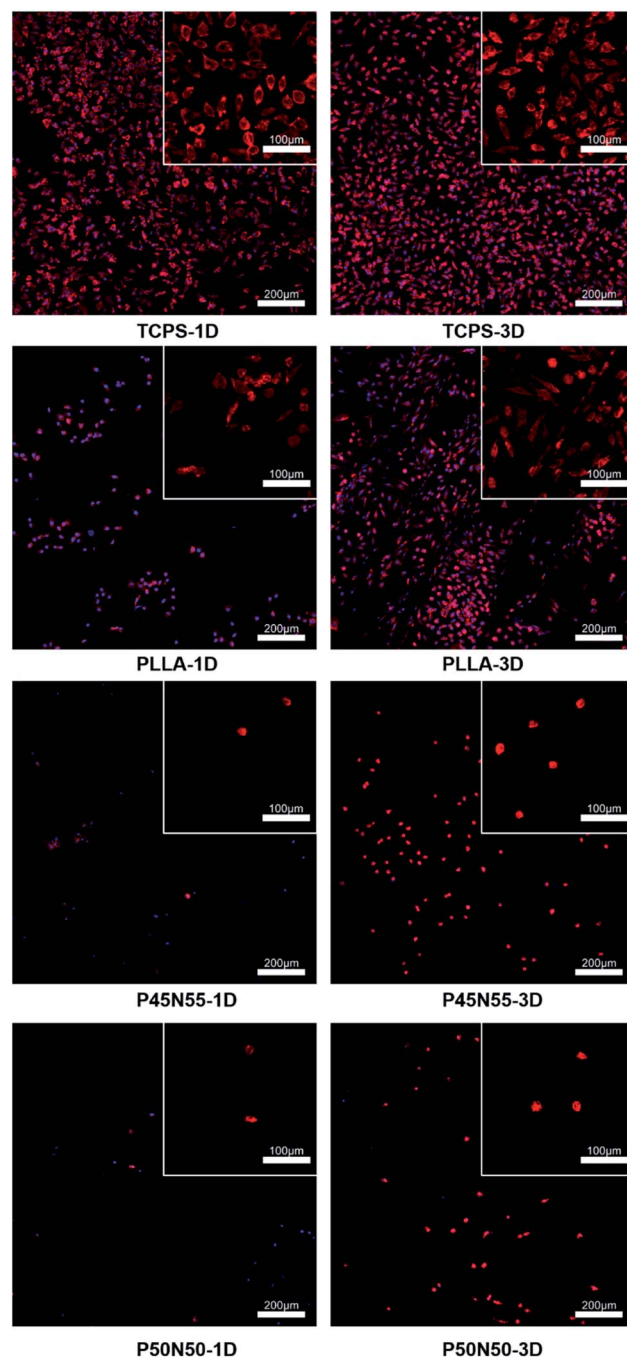

Fig. 7 Representative fluorescent micrographs of TRITC-phalloidin (red) and DAPI (blue) stained of L929 fibroblasts depicting cell morphology and quantity cultured on TCPS, PLLA, P45N55, and P50N50 surfaces for 1D and 3D (upper right corner: cytoskeleton image stained with TRITC-phalloidin).

barrier to block the adhesion of proteins and cells.[30] The surface of poly(dimethylsiloxane) (PDMS) modified with PVP significantly inhibited the adsorption of fibrinogen, albumin and vitronectin, resulting in an anti-biofouling surfaces.[31] In this study, the introduction of PVP increased the hydrophilicity of the synthesized material, which was beneficial to resist the adsorption of proteins, thereby further inhibiting cell adhesion and playing an anti-biofouling effect.

4. Conclusions

Photosensitive resin has been prepared by mixing PLLA 3-FAME, the reactive diluent NVP and the photoinitiator Irgacure 2959, which could form PLLA 3-FAME/NVP network by UV curing. The characterization of the network (such as wettability, water absorption and mechanical property) could be adjusted by introducing different amounts of NVP. No obvious cytotoxicity was found in this study. Moreover, the resultant network could resist cell adhesion, because the introduction of NVP could enhance the hydrophilicity of the surface. Combined with DLP technology, there is potential to develop an anti-adhesion barrier material with the customization requirements.

Conflicts of interest

There are no conflicts to declare.

Acknowledgements

References

1 X. P. Tan, Y. J. Tan, C. S. L. Chow, S. B. Tor and W. Y. Yeong, Metallic powder-bed based 3D printing of cellular scaffolds for orthopaedic implants: A state-of-the-art review on manufacturing, topological design, mechanical properties and biocompatibility, *Mater. Sci. Eng., C*, 2017, **76**, 1328–1343.

2 Y. Nakagawa, K. I. Mori and T. Maeno, 3D printing of carbon fibre-reinforced plastic parts, *Int. J. Adv. Des. Manuf. Technol.*, 2017, **91**, 5–8.

3 J. Méndez-Ramos, J. C. Ruiz-Morales, P. Acosta-Mora and N. M. Khaidukov, Infrared-light induced curing of photosensitive resins through photon up-conversion for novel cost-effective luminescent 3D-printing technology, *J. Mater. Chem. C*, 2016, **4**, 801–806.

4 Y. C. Chiu, Y. F. Shen, K. X. Lee, S. H. Lin and Y. W. Chen, 3D Printing of Amino Resin-based Photosensitive Materials on Multi-parameter Optimization Design for Vascular Engineering Applications, *Polymers*, 2019, **11**, 1394.

5 R. Sodian, M. Loebe, A. Hein, D. P. Martin, S. P. Hoerstrup, E. V. Potapov, H. A. Hausmann, T. Lueth and R. Hetzer, Application of stereolithography for scaffold fabrication for tissue engineered heart valves, *ASAIO J.*, 2002, **48**, 12–16.

6 M. N. Cooke, J. P. Fisher, D. Dean, C. Rimnac and A. G. Mikos, Use of stereolithography to manufacture critical-sized 3D biodegradable scaffolds for bone ingrowth, *J. Biomed. Mater. Res., Part B*, 2003, **64**, 65–69.

7 S. H. Kim, Y. K. Yeon, J. M. Lee, J. R. Chao, Y. J. Lee, Y. B. Seo, M. T. Sultan, O. J. Lee, J. S. Lee and S. I. Yoon, Precisely printable and biocompatible silk fibroin bioink for digital light processing 3D printing, *Nat. Commun.*, 2018, **9**, 1620.

8 Y. Zeng, Y. Yan, H. Yan, C. Liu and J. Chen, 3D printing of hydroxyapatite scaffolds with good mechanical and biocompatible properties by digital light processing, *J. Mater. Sci.*, 2018, **53**, 6291–6301.

9 W. Y. Yeong, N. Sudarmadji, H. Y. Yu, C. K. Chua, K. F. Leong, S. S. Venkatraman, Y. C. F. Boey and L. P. Tan, Porous polycaprolactone scaffold for cardiac tissue engineering fabricated by selective laser sintering, *Acta Biomater.*, 2010, **6**, 2028–2034.

10 N. Sudarmadji, J. Y. Tan, K. F. Leong, C. K. Chua and Y. T. Loh, Investigation of the mechanical properties and porosity relationships in selective laser-sintered polyhedral for functionally graded scaffolds, *Acta Biomater.*, 2011, **7**, 530–537.

11 D. W. Hutmacher, T. Schantz, I. Zein, K. W. Ng, S. H. Teoh and K. C. Tan, Mechanical properties and cell cultural response of polycaprolactone scaffolds designed and fabricated *via* fused deposition modeling, *J. Biomed. Mater. Res.*, 2001, **55**, 203–216.

12 S. Naghieh, M. R. K. Ravari, M. Badrossamay, E. Foroozmehr and M. Kadkhodaei, Numerical investigation of the mechanical properties of the additive manufactured bone scaffolds fabricated by FDM: The effect of layer penetration and post-heating, *J. Mech. Behav. Biomed. Mater.*, 2016, **59**, 241–250.

13 G. Zhou, Q. Han, J. Tai, B. Liu, J. Zhang, K. Wang, X. Ni, P. Wang, X. Liu, A. Jiao, S. Wang, X. Li, J. Zhang and Y. Fan, Digital light procession three-dimensional printing acrylate/collagen composite airway stent for tracheomalacia, *J. Bioact. Compat. Polym.*, 2017, **32**, 429–442.

14 D. Dean, J. Wallace, A. Siblani, M. O. Wang, K. Kim, A. G. Mikos and J. P. Fisher, Continuous digital light processing (cDLP): Highly accurate additive manufacturing of tissue engineered bone scaffolds, *Virtual Phys. Prototyp.*, 2012, **7**(1), 13–24.

15 Y. He, Z. Hu, M. Ren, C. Ding, P. Chen, Q. Gu and Q. Wu, Evaluation of PHBHHx and PHBV/PLA fibers used as medical sutures, *J. Mater. Sci.: Mater. Med.*, 2014, **25**, 561–571.

16 Y. K. Joung, J. S. Lee, K. D. Park and S.-J. Lee, 6-arm PLLA-PEG block copolymers for micelle formation and controlled drug release, *Macromol. Res.*, 2008, **16**, 66–69.

17 R. Xiao, Y. Song, T. Yang, F. Huang, J. Li and L. Chi, A preliminary clinical study on absorbable screws, *J. Biomed. Eng.*, 2005, **22**, 1055–1057.

18 A. S. Pilon, The development and characterization of a bionanocomposite tissue engineering scaffold consisting

of poly(lactic acid) (PLA) and monetite for bone regeneration, *Nat. Rev. Microbiol.*, 2010, **9**, 889.

19 F. Wang, G. Guo, Q. Ma, M. Gu, X. Wu, S. Sheng and X. Wang, Investigation on the thermo-mechanical properties and thermal stability of polylactic acid tissue engineering scaffold material, *J. Therm. Anal. Calorim.*, 2013, **113**, 1113–1121.

20 G. Xu, S. Chen and X. Yan, Synthesis and Hydrophilic Performance of Poly(Lactic Acid)-Poly(Ethylene Glycol) Block Copolymers, *Am. J. Anal. Chem.*, 2016, **7**, 299–305.

21 D. Kubies, F. Rypacek, J. Kovarova and F. Lednicky, Microdomain structure in polylactide-*block*-poly(ethylene oxide) copolymer films, *Biomaterials*, 2000, **21**, 529–536.

22 C. Yamini, K. L. Shantha and K. P. Rao, Synthesis and Characterization of Poly[N-Vinyl-2-Pyrrolidone-Polyethylene Glycol Diacrylate] Copolymeric Hydrogels for Drug Delivery, *J. Macromol. Sci., Part A*, 1997, **34**, 2461–2470.

23 Y. Zhong and P. Wolf, Effects of hydrophobic unit and its distribution on solution properties of vinyl pyrrolidone and vinyl acetate copolymer, *J. Appl. Polym. Sci.*, 2015, **74**, 345–352.

24 P. Roach, D. Eglin, K. Rohde and C. Perry, Modern biomaterials: a review - bulk properties and implications of surface modifications, *J. Mater. Sci.: Mater. Med.*, 2007, **18**, 1263–1277.

25 E. Giancotti and E. Ruoslahti, Integrin signaling, *Science*, 1999, **285**, 1028–1032.

26 I. Delon and N. H. Brown, Integrins and the actin cytoskeleton, *Curr. Opin. Cell Biol.*, 2007, **19**, 43–50.

27 E. Ostuni, R. G. Chapman, R. E. Holmlin, S. Takayama and G. M. Whitesides, A survey of structureproperty relationships of surfaces that resist the adsorption of protein, *Langmuir*, 2001, **17**, 5605–5620.

28 C. Yamini, K. L. Shantha and K. P. Rao, Synthesis and characterization of poly[n-vinyl-2-pyrrolidone-polyethylene glycol diacrylate] copolymeric hydrogels for drug delivery, *J. Macromol. Sci., Part A*, 1997, **34**, 2461–2470.

29 L. C. Xu and C. A. Siedlecki, Effects of surface wettability and contact time on protein adhesion to biomaterial surfaces, *Biomaterials*, 2007, **28**, 3273–3283.

30 M. Rabe, D. Verdes and S. Seeger, Understanding protein adsorption phenomena at solid surfaces, *Adv. Colloid Interface Sci.*, 2011, **162**, 87–106.

31 Z. Wu, W. Tong, W. Jiang, X. Liu and C. Hong, Poly(n-vinylpyrrolidone)-modified poly(dimethylsiloxane) elastomers as anti-biofouling materials, *Colloids Surf., B*, 2012, **96**, 37–43.